The influence of molecular structure and aerosol phase on the heterogeneous oxidation of normal and branched alkanes by OH

Christopher R. Ruehl[1,2], Theodora Nah[1,3], Gabriel Isaacman[2], David R. Worton[2,4], Arthur W. H. Chan[2], Katheryn R. Kolesar[5], Christopher D. Cappa[5], Allen H. Goldstein[2,6,7], and Kevin R. Wilson[1]*

[1] *Chemical Sciences Division, Lawrence Berkeley National Laboratory, Berkeley, CA 94720, USA*

[2] *Department of Environmental Sciences, Policy, & Management, University of California, Berkeley, CA 94720, USA*

[3] *Department of Chemistry, University of California, Berkeley, CA 94720, USA*

[4] *Aerosol Dynamics Inc., Berkeley, CA 94710, USA.*

[5] *Department of Civil & Environmental Engineering, University of California, Davis, CA 95616, USA*

[6] *Department of Civil & Environmental Engineering, University of California, Berkeley, CA 94720, USA*

[7] *Environmental Energy Technologies Division, Lawrence Berkeley National Laboratory, Berkeley, CA 94720, USA*

* Correspondence to: krwilson@lbl.gov

ABSTRACT:

Insight into the influence of molecular structure and thermodynamic phase on the chemical mechanisms of hydroxyl radical-initiated heterogeneous oxidation is obtained by identifying reaction products of submicron particles composed of either *n*-octacosane ($C_{28}H_{58}$, a linear alkane) or squalane ($C_{30}H_{62}$, a highly branched alkane) and OH. A common pattern is observed in the positional isomers of octacosanone and octacosanol, with functionalization enhanced towards the end of the molecule. This suggests that relatively large linear alkanes are structured in submicron particles such that their ends are oriented towards the surface. For squalane, positional isomers of first-generation ketones and alcohols also form in distinct patterns. Ketones are favored on carbons adjacent to tertiary carbons, while hydroxyl groups are primarily found on tertiary carbons but also tend to form towards the end of the molecule. Some first-generation products, viz., hydroxycarbonyls and diols, contain two oxygen atoms. These results suggest that alkoxy radicals are important intermediates and undergo both intramolecular (isomerization) and intermolecular (chain propagation) hydrogen abstraction reactions. Oxidation products with carbon numbers less than the parent alkane are observed to a much greater extent for squalane than for *n*-octacosane oxidation and can be explained by the preferential cleavage of bonds involving tertiary carbons.

1. Introduction

The heterogeneous oxidation of atmospheric organic aerosols can transform particulate properties with a direct influence on climate, human health and visibility. Previous work has attempted to estimate the relative importance of different oxidation pathways by distilling the complex chemistry involving free radical intermediates into two generalized reaction pathways, termed functionalization and fragmentation. Functionalization occurs when an oxygenated functional group is added to a molecule, leaving the carbon skeleton intact. Alternatively, fragmentation involves C–C bond cleavage and produces two oxidation products with smaller carbon numbers than the reactant. The ability to predict secondary organic aerosol (SOA) yields, and thus ambient SOA concentrations, is very sensitive to the assumed "branching ratio" between functionalization and fragmentation. This is because functionalization produces less volatile compounds and increases particulate mass, while fragmentation typically forms more volatile products that can evaporate and thereby decrease particulate mass. A third general type of pathway, oligomerization, reduces average volatility and increases carbon number, and is thus similar to functionalization in its impact on organic aerosol formation and aging. The potential utility of representing aerosol formation and aging chemistry in models using these "generalized reaction pathways" relies on developing parameterizations that are experimentally validated through detailed measurements of oxidation products.

Much more is known about the chemistry of free radical-induced hydrocarbon oxidation in the gas phase than in the condensed phase.[1] Gas-phase mechanisms and product branching ratios are often used as a starting point (including in this study) when investigating heterogeneous oxidation, in an effort to identify key similarities and/or differences between heterogeneous and gas-phase oxidation rates and mechanisms. The reaction between a saturated

organic molecule and OH begins with the abstraction of a hydrogen atom to form an alkyl radical, which in the presence of O_2, forms a peroxy radical as shown in Fig. 1a. In the absence of NO and HO_2, peroxy radicals undergo self-reactions following one of two general pathways, which form stable products and/or alkoxy radicals. The pathway that forms stable products in the condensed phase includes (at least) two specific mechanisms. Peroxy radicals can react via the Russell mechanism to form a carbonyl-containing compound (either an aldehyde or a ketone), and an alcohol, with O_2 formed as a co-product.[2] The self reaction can also proceed via the Bennett-Summers mechanism to form two carbonyls and H_2O_2.[3]. Alternatively, two alkoxy radical intermediates and O_2 can be formed via self-reaction, opening up a variety of possible subsequent reaction pathways.

Gas phase alkoxy radicals, under atmospheric conditions, react in one of three ways:[4] hydrogen abstraction, decomposition by β-scission, and ketone formation via reaction with O_2 (Fig. 1b). Intramolecular hydrogen abstraction results by isomerization; intermolecular hydrogen abstraction leading to chain propagation is also possible, perhaps even more so in the condensed phase where concentrations are locally very high. Isomerization proceeds most rapidly via a 1,5 H shift (i.e., abstraction of a H atom from the δ-C atom) through a relatively low-strain six-member cyclic transition state. Evidence for this pathway in the gas phase includes observations of pentanone isomers formed from the photooxidation of pentane.[5] Similar observations of hexane photooxidation products indicate that 1,4 H shifts (involving five-membered cyclic transition states) are of negligible importance relative to 1,5 H shifts.[6] Photooxidation experiments on larger gas-phase *n*-alkanes have shown that isomerization reactions increase in importance (and that of scission reactions decreases) with carbon chain length.[7, 8] It remains unclear how these detailed gas phase mechanisms, formulated for relatively small molecules, can

78 be applied to heterogeneous free radical oxidation of larger organic molecules in aerosol
79 particles.

80 Early studies of heterogeneous chemistry focused on inorganic compounds, and some of
81 the first identified atmospherically-relevant reactions involve nitrogen and/or chlorine containing
82 compounds on sea salt aerosol[9] or in polar stratospheric clouds.[10] Recently, heterogeneous
83 oxidation of organic aerosols (OA) has received increased attention.[11, 12, 13] Most studies have
84 shown that heterogeneous oxidation of organic compounds is about as efficient as gas-phase
85 oxidation, assuming there is sufficient time for gas-phase oxidants to diffuse to the surfaces of
86 condensed phases. The heterogeneous rate is typically expressed as an uptake coefficient or
87 reaction probability (γ), which is the fraction of collisions between gas-phase oxidants and a
88 condensed phase, or a specific condensed-phase molecule, that result in a reaction. One of the
89 most important of these gas phase oxidants is the hydroxyl (OH) radical, and OH uptake
90 coefficients (γ^{OH}) have been reported both for films and microscopic particles. For example, γ^{OH}
91 = 0.34 was measured for thin paraffin wax films[14] and $\gamma^{OH} > 0.2$ for hexanol adsorbed onto water
92 ice surfaces[15], based on gas-phase OH decay. More recently, OH uptake coefficients based on
93 measured particle-phase decay of specific compounds ranging from 0.37 to 0.51 were reported
94 for more oxygenated single-component organic particles such as citric acid,[16] and values
95 between 0.77 and 1.04 for erythritol and levoglucosan,[17] palmitic acid,[18] and hexacosane
96 particles.[19] Larger γ^{OH} values of 1.3[20] and 2.0[21] have been observed for free radical oxidation of
97 bis(2-ethylhexyl) sebacate particles in a flow tube. Observations of $\gamma^{OH} > 1$ indicate an important
98 role for secondary radical chain chemistry (although even when $\gamma^{OH} < 1$ such chain chemistry
99 may still be important). Values larger than 3 were observed for the reaction of squalane particles
100 with Cl atoms in the absence of O_2.[22] Although these studies have provided much insight into

heterogeneous reaction rates, there are comparably fewer studies that have examined the resulting distribution of oxidation products produced in these reactions. Such measurements are essential to the identification of important heterogeneous reaction mechanisms.

Several previous studies have investigated the relative importance of functionalization and fragmentation pathways in the oxidation of organic matter. In the gas phase, the decomposition rate of alkoxy radicals (i.e., fragmentation) depends on the stability (i.e., the ionization energy) of the alkyl radical created by the C-C bond scission.[23] While fragmentation pathways are well-established in the gas-phase, previous studies have come to conflicting conclusions about the relative importance of fragmentation in heterogeneous reactions. Some studies have found that fragmentation is an important pathway leading to rapid carbon loss from organic films[24,25] or aerosol particles.[18] Volatilization of oxidation products was observed to decrease the volume of bis(2-ethylhexyl) sebacate (BES) aerosol by ~20% after ~2 OH lifetimes.[20] This is in contrast to a study of NO_3-initiated oxidation of oleic acid (C_{18}) aerosol, which observed no C_9 aldehyde formation (i.e., the fragmentation product expected based on the position of the double bond in oleic acid). This indicates, for this system of liquid particles, functionalization (e.g., the Russell mechanism) dominates the peroxy radical self-reaction.[26] This agrees with a study of the NO_3-initiated oxidation of thin saturated hydrocarbon films, which also resulted in minimal fragmentation.[27] Changes in particle phase may be playing a role in these discrepancies, but it is currently not clear how important this effect might be.

Some previous work has identified specific products of radical-initiated heterogeneous oxidation to reveal the importance (or lack thereof) of certain chemical mechanisms. For example, a previous study of the heterogeneous oxidation of a hexadecane film by OH identified all positional isomers of hexadecanone (i.e., functionalization products), as well as short-chain

aldehydes and carboxylic acids (i.e. fragmentation products).[28] However, no alcohol products were detected, which was attributed to a small branching ratio to the Russell mechanism. An excess of ketones relative to alcohols was observed during the heterogeneous radical-initiated oxidation of dioctyl sebacate aerosol, suggesting an alternative pathway to the Russell mechanism, such as the Bennett-Summers pathway or alkoxy radical formation.[29] On the other hand, in a study of NO_3-initiated oxidation of oleic acid (C_{18}) particles found that the Russell mechanism (i.e., functionalization) is dominant and that the branching ratio to form alkoxy radicals (which can fragment) is of minimal importance.[26]

In addition to investigations of the heterogeneous oxidation products of different model compounds, the importance of aerosol phase (i.e., solid vs. liquid) has also been examined. The Cl atom initiated oxidation of supercooled liquid and solid brassidic acid ($C_{22}H_{42}O_2$) particles, revealed that liquid particles reacted slightly more rapidly. However, the volume of solid particles decreased to a greater extent upon reaction, suggesting greater fragmentation and subsequent evaporation than for liquid particles.[30] A similar increase in the production of volatile gas phase molecules was observed for OH-initiated heterogeneous oxidation of solid steric acid films relative to liquid BES films.[25]

The two hydrocarbon precursors used in this work, squalane (a liquid branched alkane) and octacosane (a solid normal alkane), are relatively non-volatile (boiling points of 176 and 343ºC, respectively), and thus have been used in previous studies of particle-phase hydrocarbon oxidation.[31, 32, 33] Here these two compounds are used to explore how aerosol phase and/or differences in molecular structure (i.e. branching of the carbon skeleton) alter the reaction product distributions produced by heterogeneous oxidation. Previously, it was found that the squalane + OH reaction could be well described by the multigenerational formation and

147 evolution of reaction products described as a Poisson distribution.[34] While these studies have
148 provided a general description of the reaction, finer details are needed to develop new molecular
149 and mechanistic insights into how functionalization and fragmentation pathways depend upon
150 molecular structure and/or aerosol phase.

151 Although previous work has focused broadly on describing how multiple generations of
152 reaction products evolve during heterogeneous oxidation, here we primarily focus on the
153 molecular and positional isomeric distribution of first generation oxidation products. Single-
154 component aerosols (either squalane or octacosane) are photo-oxidized in a flow tube reactor and
155 the reactions products are analyzed using two-dimensional gas chromatography coupled to mass
156 spectrometry. Analytes are ionized either with vacuum ultraviolet (VUV, 10.5 eV) photons or by
157 electron impact (EI, 70 eV). This approach provides a way to examine how the formation of
158 specific oxidation products depends upon aerosol phase and molecular branching structure.
159 Specifically we determine how the location of a carbon atom along the molecular backbone
160 relates to its propensity to functionalize (i.e., the distribution of positional isomers of
161 functionalization products). Furthermore, for fragmentation reactions, the most likely carbon-
162 carbon bonds to cleave are identified by examining the carbon number distribution of the
163 oxidation products. These results provide the molecular details to better refine heterogeneous
164 reaction mechanisms, which provide the fundamental basis for more realistic parameterizations
165 of functionalization and fragmentation pathways in organic aerosols.

166 2. Experimental

167 Pure hydrocarbon particles are formed via homogeneous nucleation using an oven heated
168 to 120-130 ºC. The aerosol is then passed through an annular charcoal denuder to remove

residual gas phase species from the flow. The particles are then mixed with humidified N_2, O_2, and O_3, and sent to a flow-tube reactor as described in detail in previous publications.[31, 32] The reactor is comprised of a 1.3m long, 2.5cm ID type-219 quartz tube, surrounded by mercury lamps which produce light with a peak wavelength of 254 nm. O_3 is produced by passing O_2 through a corona discharge ozone generator. OH concentration is varied by changing the O_3 concentration in the reactor (maximum [O_3] was 1000 ppb). The relative humidity in the reactor is kept at 30%, and the total flowrate at 1 lpm, resulting in an average residence time in the flow tube of ~37s. With all the lights off (i.e., when OH exposure was zero), the octacosane and squalane particles have concentrations of 11,000 and 6,500 μg m^{-3} and surface-weighted mean diameters (D_{surf}) of 282 and 164 nm, respectively. Under these conditions, heterogeneous processes (relative to gas phase oxidation) are expected to dominate, due to the high particle loading and surface-to-volume ratios.[11]

During flow tube experiments, samples are collected onto quartz filters (47 mm Tissuquartz, Pall Life Science) which were pre-baked at 600 °C for at least 6 hours to remove organic contaminants. Immediately before collection, gas-phase compounds are removed from the samples by a charcoal denuder (8 in. 480-channel MAST Carbon). Samples are collected at OH exposures ([OH] × time) ranging from 0 to 5.8 × 10^{12} molec cm^{-3} s, as determined by the observed decay of the gas phase tracer hexane. The air volume sampled varies from 4.5 to 20 L, to achieve filter concentrations of 1.1 to 3.7 μg C cm^{-2}. Filter punches (1.6 cm^2) are thermally desorbed at 320°C under helium using a thermal desorption system and autosampler (TDS3 & TDSA2, Gerstel). Desorbed samples are focused at 20°C on a quartz wool liner in a cooled injection system (CIS4, Gerstel) before they are introduced into a two-dimensional gas chromatograph (GC×GC, Agilent 7890). All filters are analyzed using 70 eV electron impact

(EI) as an ionization source. A subset of these filters (for each parent compound, one at ~1 and one at ~3 OH lifetimes) are analyzed using soft (10.5 eV) vacuum ultraviolet (VUV) photons at the Advanced Light Source (ALS), Lawrence Berkeley Laboratory (extracted single-ion chromatograms shown in Figs. S1-4). These measurements involve a custom modification of the mass spectrometer ion source to facilitate direct coupling to the ALS.

For both VUV and EI ionization sources, comprehensive GC×GC analysis is performed using a 60 m × 0.25 mm × 0.25 μm non-polar capillary column (Rxi-5Sil MS, Restek) for the first-dimension separation (by volatility), and a medium-polarity second dimension column (1 m × 0.25 mm × 0.25 μm, Rtx-200MS, Restek). A dual-stage thermal modulator (Zoex), consisting of a guard column (1 m × 0.25 mm, Rxi, Restek) and with a modulation period of 2.4 s, is used as the interface between the two columns. Mass spectra are obtained with a high-resolution ($m/\Delta m$ = 4000) time-of-flight mass spectrometer (HTOF, ToFWerk). An example EI chromatogram is shown in Fig. 2. The VUV results, which feature a larger signal at the parent m/z ratio and fewer ion fragment peaks (Fig. 3), are used to identify specific compounds, including positional isomers, in the chromatogram. For the detection of alcohols and acids, all filters are also subjected to *in situ* gas-phase derivatization facilitated by sweeping the headspace of a vial filled with *N*-Methyl-*N*-(trimethylsilyl) trifluoroacetamide (MSTFA) during the thermal desorption cycle. Comparison of derivatized and underivatized chromatograms indicate that tertiary alcohols dehydrated during desorption (i.e., before chromatography) and were detected as alkenes. For example, tertiary "squalanols" ($C_{30}H_{62}O$) appear as derivatized alcohols ($C_{33}H_{70}OSi$) when MSTFA was used, but as alkenes ($C_{30}H_{60}$) in the absence of MSTFA. Dehydration of tertiary alcohols is confirmed with authentic standards of tertiary alcohols including 3,7-dimethyl-3-octanol and 4-terpeneol.

The decay of both octacosane and squalane are quantified both by the total EI signal and the 12 most prominent $C_nH_{2n+1}^+$ EI fragments. The decay constants (k_{parent}) obtained from exponential fits to the decay of octacosane or squalane are used to compute uptake coefficients (γ_{parent}^{OH}), by normalizing the rate of parent decay to the OH-particle collision rate,[32] while correcting for the limitations to reaction rate due to gas-phase diffusion of OH to the particle surface.[35] Kinetic lifetimes (τ) are computed using the first-order decay constants of squalane or octacosane (i.e $\tau = k_{Parent}[OH]t$). Analytical standards are not available for the early oxidation products of squalane and octacosane, thus adding to the uncertainty in their quantification. In most GC systems (including ours), the response factors tend to decrease with both decreasing volatility and increasing polarity. As an upper limit for the response factor, deuterated *n*-alkanes are used to correct for the volatility response. As a lower limit, we also account for the polarity by multiplying the upper limit response factor by the ratio of the response of anthraquinone to *n*-eicosane, two deuterated internal standards with similar volatilities but different polarities. This is considered a lower limit since the difference in both the number of O atoms and O:C ratio is greater between anthraquinone and eicosane than it is between first-generation oxidation products and squalane/octacosane. Authentic standards for several octadecanone isomers (2-, 3-, 5-, and 9-octadecanone) are used to correct the response factors for equivalent octacosanone isomers. Standards of 2- and 3-tridecanone as well as tridecanal are used to correct the response factors of aldehydes relative to ketones.

3. Results and Discussion

In Section 3.1 the oxidation kinetics of octacosane and squalane will be presented and compared. Oxidation product identification for octacosane and squalane are detailed in sections

237 3.2 and 3.3, respectively. These final two sections are further subdivided into functionalization
238 (3.*n*.1) and fragmentation (3.*n*.2) products.

239 3.1 Oxidation Kinetics

240 The total octacosane EI signal decays with OH exposure, with an average first-order
241 decay constant of $4.2 \pm 2.2 \times 10^{-13}$ molec^{-1} cm^3 s^{-1} (Fig. 4a, uncertainty indicates 90% confidence
242 intervals of the exponential fit). All individual $C_nH_{2n+1}^+$ EI fragments are within this uncertainty
243 range, which is equivalent to an uptake coefficient of 0.18 ± 0.11. Squalane decreases with OH
244 exposure, with a decay constant of $1.6 \pm 0.4 \times 10^{-12}$ molec^{-1} cm^3 s^{-1} (Fig. 4b). This yields an
245 uptake coefficient of 0.36 ± 0.11, indicating that squalane is oxidized twice as quickly as
246 octacosane. This value is slightly larger than the previously reported value of 0.30 ± 0.07,[32] and
247 the larger uncertainty for the measurement reported here arises from the relatively few (six) data
248 points used to calculate the squalane decay.

249 Possible explanations for the larger γ^{OH} for squalane than octacosane can be understood
250 by comparing the timescales of the different processes that influence the oxidation kinetics under
251 the conditions of this reaction. The self-diffusion coefficient of squalane is 7×10^{-7} cm^2 s^{-1},[36]
252 which (for a 164 nm particle) is equivalent to a mixing timescale of 10^{-5} s.[26] The timescale for
253 the reactive loss of squalane to OH radicals (i.e., the ratio of the squalane decay constant to the
254 average [OH] in the reactor) is approximately 20 s.[26] Because the timescale for diffusion in the
255 squalane particle is a factor of $\sim 2 \times 10^5$ shorter than that of the reaction timescale, it can be
256 assumed that unreacted squalane is continuously replenished at the surface of these microscopic
257 particles. In contrast, diffusion coefficients for semi-solids and solids are expected to be below
258 10^{-10} cm^2 s^{-1},[37] and therefore the timescale of mixing in solid octacosane particles will be much

closer to the reaction timescale. This suggests that the diffusion of unreacted material to the particle surface may limit the overall rate at which octacosane reacts with OH. A more subtle difference in the decay of the parent ion signals is consistent with this difference in phase. The squalane decay is better described as single exponential (Fig. 4b), whereas octacosane appears to react more quickly during the first oxidation lifetime and then more slowly as oxidation proceeds (Fig. 4a). This could be consistent with a kinetic delay associated with surface replenishing of octacosane molecules.

In addition to differences in phase, the more rapid heterogeneous oxidation of squalane relative to *n*-octacosane could also be due to more rapid hydrogen abstraction from the tertiary carbons present in squalane (*n*-octacosane, a linear alkane, has no tertiary carbons, while squalane has six). Previous studies of the reactivity of different carbon atoms (primary, secondary, and tertiary) for gas phase hydrocarbons are summarized in so-called Structure Reactivity Relationships (SRR), and indicate that tertiary carbons are more reactive than secondary or primary carbons.[38] A previous investigation into the heterogeneous oxidation of motor oil using similar analytical techniques concluded that this enhanced reactivity associated with tertiary carbons (i.e., branching in the carbon backbone) is more pronounced in heterogeneous oxidation than it is in the gas phase.[39]

3.2 Octacosane

3.2.1 Functionalization products

The majority of the observed octacosane oxidation products are the result of functionalization reactions, including $C_{28}H_{56}O$ compounds (i.e., various octacosanone isomers and octacosanal). The sum of the concentrations of $C_{28}H_{56}O$ isomers reaches a maximum value

of 45 ± 18 μg m^{-3} at an OH exposure of 1.2 × 10^{12} molec cm^{-3} s (approximately 0.5 lifetimes). Similar concentrations of $C_{28}H_{58}O$ compounds (i.e., octacosanols) are observed. The observed fragmentation products (with carbon numbers less than 28) are minor in comparison, with a maximum uncertainty range of less than 5 μg m^{-3} (Fig. 4a).

All single-carbonyl compounds (octacosanal and 2- through 14-octacosanone) are detected and chromatographic separation is achieved for all these isomers up to 8-octacosanone. The total EI signal intensity could not be used to individually quantify the 9- through 14-octacosanone isomers since they co-elute. The closer the carbonyl is to the end of the molecule, the greater the GC retention time, with relatively large gaps between 2-, 3-, and 4-octacosanone, but smaller gaps between subsequent octacosanone isomers (Fig. S1). This is in agreement with a previous GC/MS analysis of heterogeneous oxidation of hexadecane films by OH,[28] as well as the analysis of an isotopic mixture of authentic octadecanone standards.

Shown in Fig. 5a is the distribution of octacosanone isomers, which reveals a clear enhancement in the formation of the carbonyl group towards the terminus of the molecule. While the ketone groups formed at carbon positions greater than 5 are formed with similar yields, 5-, 4-, 3-, and 2-octacosanone are enriched relative to the more interior ketones by factors of 1.5, 2.2, 4.8, and 10, respectively (Fig. 5a). The yield of octacosanal is smaller than that of the interior ketones. A similar pattern is observed for the positional isomers of octacosanol as shown in Fig. 5b.

Previous studies of the reactivity of different carbon atoms (primary, secondary, and tertiary) for gas phase hydrocarbons are summarized in SRR predictions,[38] shown explicitly in Figs. 5a and b. The rate of hydrogen abstraction from terminal carbons is expected to occur ten

303 times more slowly than from more interior carbons, which helps explain the observed low yields
304 of octacosanal and *n*-octacosanol. SRR, however, also predicts that the hydrogen abstraction rate
305 from the secondary carbon atoms adjacent to terminal carbons should occur about 20% more
306 slowly than from those carbons atoms located towards the interior of the molecule. This is in
307 contrast to the observed isomer distribution, which exhibits a pattern nearly opposite of that
308 predicted by SRR. This suggests that more subtle features of the aerosol (e.g., phase or molecular
309 orientation at the particle surface) are playing a more dominant role in the reaction than
310 differences in the reactivity of individual carbon atoms within the molecule.

311 One explanation for the positional isomer pattern is that octacosane molecules at the
312 interface are preferentially oriented with their carbon backbones normal to the aerosol surface.
313 This is consistent with "surface freezing" of *n*-alkanes, in which these hydrocarbon molecules
314 adopt more ordered configurations at the interface.[40] Furthermore, molecular dynamics
315 simulations show that the terminal carbons of liquid *n*-alkanes are enhanced at the interface.[41, 42]
316 Such a surface orientation would lead to an enhanced encounter frequency of an OH radical with
317 the terminal carbons of *n*-octacosane and is consistent with the observed carbonyl and alcohol
318 isomer distributions, shown in Fig. 5.

319 3.2.2 Fragmentation products

320 Analysis of the chromatogram shown in Fig. 2 reveals very low yields of octacosane-
321 derived fragmentation products (i.e., formed by breaking C-C bonds). As shown in Fig. 6,
322 several *n*-alkanoic acids up to octacosanoic (C_{28}) acid are detected at concentrations of ~1 μg m^{-3}
323 . At low OH exposures, *n*-alkanoic acid concentrations increase for carbon numbers larger than
324 22. Hexacosanoic (C_{26}) acid is formed in the largest relative yield, suggesting that breaking the
325 second C-C bond is more favorable than the terminal C-C bond. At higher OH exposures, a

preference for even-numbered acids provides further evidence for enhanced cleavage of the second (relative to the terminal) C-C bond. Octacosanoic acid is the most prevalent acid at higher OH exposures, suggesting that it is formed as a second- or higher-generation product. Conversion of aldehydes to acids during the heterogeneous oxidation of thin films has previously been observed,[25] which could explain the increase in the relative importance of octacosanoic acid at higher OH exposures.

Octacosane fragmentation reactions can explain only a small part of the rapid decrease in the volume of octacosane particles measured by the SMPS (54% over ~1 oxidation lifetime, Fig. 4a). Alternatively, most of the SMPS volume decrease could be related to a decrease in mobility diameter associated with a particle shape or density change induced by oxidation. A decrease in the shape factor from an initial value of 1.3 to 1 would explain the entirety of this 54% decrease in volume. Thus, while alkanoic acid fragmentation products are observed (Fig. 6), and fragmentation reactions have been observed in other studies of solid hydrocarbons,[24, 30, 25] C-C bond scission is much less significant for octacosane relative to squalane (discussed below).

3.3 Squalane

3.3.1 Functionalization products

The observed concentrations of squalane oxidation products are much higher than those of octacosane at a given oxidation lifetime. The sum of "squalanone" (2,6,10,15,19,23-hexamethyltetracosan-*n*-one) concentrations reaches a maximum of 297 ± 120 μg m^{-3} after an OH exposure of 5.5 × 10^{11} molec cm^{-3} s (approximately 0.9 lifetimes), as shown in Fig. 4b. Using the VUV chromatograms for individual $C_nH_{2n+1}O^+$ ion fragments, six squalanone isomers are isolated, with the two remaining isomers (9- and 12-squalanone) co-eluting (Fig. S3). Similar

concentrations and kinetics are observed for squalanol, with twelve positional isomers isolated by VUV-MS (Fig. S4).

As shown in Fig. 7a, carbonyls on carbon atoms adjacent to tertiary carbons are formed in the highest abundance. The EI signal for these "α-carbonyls" is about five times larger than for the "β-carbonyls" (i.e., carbonyls on atoms separated from tertiary carbons by one intermediate carbon). Standards for branched ketone isomers are not available, and therefore the assessment of this ketone isomer pattern is not as quantitative as the octacosanone isomer pattern discussed above. However, the similarity in total EI signal with those of individual fragment ions (e.g., $C_4H_9^+$, the formation of which would not be expected to depend strongly on the location of a single carbonyl group on a C_{30} compound) provides additional confidence in our observation that α-carbonyls are enriched relative to β-carbonyls. As with the sum of these compounds, the individual ketone isomers reach a maximum at an OH exposure of 5.5×10^{11} molec cm^{-3} s (i.e., ~0.9 lifetimes, Fig. 4b), indicating that these species are first generation oxidation products.

SRR predicts that H-abstraction should be equally rapid for the α- and β-carbons of squalane (Fig. 7a), since they are both secondary.[38] This suggests that the observed enrichment of the α- over the β-carbonyls is due to differences in the subsequent chemistry of the peroxy or alkoxy radicals formed at these different carbon sites. Peroxy radicals formed at these α- and β-positions can both form carbonyls via the Russell mechanism. If these peroxy radicals are converted to alkoxy radicals, however, they can abstract a hydrogen from either the same molecule (isomerization) or another molecule (chain propagation), which converts the alkoxy radical into a hydroxyl group (Fig. 1b). Because isomerization generally involves a six-membered cyclic transition state, β-alkoxy radicals have more hydrogen atoms available for abstraction than α-alkoxy radicals, as shown in Fig. 8. It is therefore likely that this pathway is

371 enhanced for β-carbons, resulting in less efficient ketone formation at these sites. Further
372 evidence for this pathway is observed in the kinetic evolution of multi-functional products with
373 two oxygen atoms, discussed below. A difference in the O_2 reactivity of these isomers is much
374 less likely, and while fragmentation is an important pathway for these squalane oxidation
375 experiments (if only at higher OH exposures), it would tend to suppress squalanone formation at
376 the α-carbons. It is also possible that β-alkoxy radicals more readily abstract H atoms from other
377 molecules, as this would also inhibit squalanone formation at β-carbons. We conclude that the
378 distribution of first-generation ketones in radical-initiated squalane oxidation is not controlled
379 solely by rate of H abstraction but is also governed, in part, by intra- and/or intermolecular
380 hydrogen abstraction pathways via alkoxy radical intermediates.

381 In contrast to the linear alkane, the distribution of squalanol isomers (Fig. 7b) is different
382 than what is observed for squalanones. The preference for α- over β-carbons for hydroxyl
383 functionalization is much less pronounced. The most prevalent isomers, 2-, 6-, and 10-squalanol,
384 can be explained by more rapid initial H abstraction rates from these tertiary carbons consistent
385 with SRR predictions shown in Fig. 7b. There is also, however, an overall enrichment in alcohol
386 functional groups formed toward the end of the molecule, which is not captured by SRR
387 calculations. The origin of this enrichment is currently unknown, but could be due to the
388 branching ratio of intra- to intermolecular H abstraction by alkoxy intermediates (Fig. 1b). If
389 alkoxy radicals towards the end of the molecule are more exposed to other molecules, they might
390 be more likely to undergo intermolecular H abstraction, yielding squalanols. More interior
391 alkoxy radicals may instead be more likely to undergo intramolecular H abstraction, which
392 would lead to multi-functional compounds, discussed below.

Several products containing two oxygenated functional groups are also detected. The identification of the parent ion in the VUV mass spectra, combined with both GC retention times, allows these compounds to be classified into three groups: $C_{30}H_{62}O_2$ ("squaladiols"), $C_{30}H_{60}O_2$ ("hydroxysqualanones"), and $C_{30}H_{58}O_2$ ("squaladiones"). The first two groups do not include alkanoic acids, which have distinct mass spectra. Figure 9 depicts the kinetic evolution of these three groups. All squaladiones (two carbonyl groups) compounds are second- or higher-generation products and are thus formed via multiple reactions with OH (Fig. 9c). Most squaladiols (two OH groups, Fig. 9a) and approximately half the hydroxysqualanones (Fig. 9b), however, have a kinetic evolution that is consistent with first generation products. The formation of two oxygenated functional groups by a single OH reactive collision can occur via isomerization (discussed above). Thus the presence and kinetic evolution of these species supports the interpretation that intramolecular hydrogen abstraction by alkoxy radicals is an important pathway during the heterogeneous oxidation of squalane. As suggested by Fig. 7b, alkoxy radicals formed on terminal carbon atoms are more likely to abstract a hydrogen atom from a neighboring molecule, implying that these first-generation bi-functional compounds are produced predominantly from alkoxy radicals centered on interior carbons.

3.3.2 Fragmentation products

In contrast to octacosane, significant quantities of squalane fragmentation products (i.e., particle-phase molecules containing less than 30 carbon atoms) are formed during the reaction. The sum of the concentrations of these compounds is 154 ± 71 μg m^{-3} at ~0.9 lifetimes (Fig. 4b), which is approximately half the quantity of first-generation carbonyl functionalization ($C_{30}H_{60}O$) products. As shown in Fig. 10, identified fragmentation products in non-derivatized samples include 33 carbonyls ($C_nH_{2n}O$), 32 lactones ($C_nH_{2n-2}O_2$), 57 alcohols (detected as C_nH_{2n}), and 40

hydroxycarbonyls (detected as $C_nH_{2n-2}O$). These classifications are based upon knowledge of exact parent molar masses and 2nd dimension (polarity) GC retention times. The most common carbon number of the fragmentation products is 24 (this was true of several compound classes). Other prevalent carbon numbers, in order of decreasing abundance, are 19, 22, 13, 11, and 17 (Fig. 10a). Assuming that only one C–C bond is broken in these reactions, this indicates that bonds involving tertiary carbons are the most likely to be cleaved.

This analysis does not detect molecules with fewer than ~8 carbon atoms, although the decrease in squalane particle volume limits the yield of such species to < 7% at one lifetime. Previous studies of the squalane system conducted by our group have found that at low OH exposures, oxidation is dominated by functionalization, while fragmentation becomes increasingly important as OH exposure increases, equaling functionalization after approximately 3 squalane oxidation lifetimes.[31, 34] Most of the products measured here reach their maxima between 1 and 2 kinetic lifetimes, and thus the 2:1 functionalization:fragmentation branching ratio of this study is consistent with previous work. The lack of fragmentation in linear octacosane (Fig. 6a), along with the strong preference for squalane fragmentation products formed via cleavage of a C-C bond involving a tertiary carbon (Fig. 10a), suggests that the heterogeneous functionalization:fragmentation branching ratio depends strongly on the amount of branching in the parent hydrocarbon. Lower aerosol yields have been observed for branched alkanes in the gas phase, which is also likely due to enhanced fragmentation relative to linear alkanes.[43]

The observation that the bonds in squalane most susceptible to cleavage involve tertiary carbons is expected, since β-scission of an alkoxy radical produces an alky radical (Fig. 1b) and an α-alkoxy radical would produce a more stable secondary alkyl radical. This preference is not

reflected in the squalanone isomer pattern because a preference for fragmentation of α- over β-alkoxy radicals would, for functionalization products, tend to favor formation of β- over α-ketones. This is likely due to the relatively low OH exposures examined in this study, under which functionalization dominates fragmentation. It is quite possible that at higher OH exposure (i.e., higher generations), the fragmentation pathway (i.e., β-scission) will have similar or even greater influence than functionalization pathways (i.e., isomerization vs. reaction with O_2) on the isomeric distribution of squalane heterogeneous oxidation products.

The temporal evolution of the fragmentation product classes is consistent with previous studies of this system. OH-initiated heterogeneous oxidation of squalane tends to add an average of one O atom per molecule for each squalane oxidation lifetime.[32] Thus, it is expected that carbonyl ($C_nH_{2n}O$) compounds and alcohols (detected as C_nH_{2n}) are first-generation products (Fig. 10b). Two other classes, $C_nH_{2n-2}O_2$ (here called "lactones" based on similarities to compounds in EI-MS libraries) and hydroxycarbonyls (detected as $C_nH_{2n-2}O$), both peak at higher OH exposures, suggesting that they originate from second- or higher-generation products.

4. Conclusions

The OH-initiated heterogeneous oxidation of squalane aerosol is approximately two times faster than for octacosane (uptake coefficients of 0.41 ± 0.11 and 0.18 ± 0.11, respectively). This is likely due at least in part to the differences in the aerosol phase. Squalane is a liquid at room temperature, and thus unreacted squalane is likely rapidly replenished at the surface of these particles. In contrast, octacosane is a solid, and thus diffusion of molecules from the interior to the surface is expected to be many orders of magnitude slower. Although octacosane reacts more slowly than squalane, the octacosane volume determined from measured particle mobility

diameter (assuming spherical particles) decreased much more rapidly than for squalane particles (54% vs. 7% over one oxidation lifetime). While this could partially be caused by evaporation of fragmentation products, it is likely largely due to an increase in density and/or a decrease in particle shape factor for the aerosol as it is oxidized.

The influence of the phase of the particle is observed in the distribution of octacosanone and octacosanol positional isomers, which are the most prominent first-generation products observed during octacosane oxidation. All functionalization of interior carbons (i.e., 6- through 14-octacosanone/ol) occurs with similar albeit small yields. The ketones and alcohols formed at the end of the molecule, however, are enriched compared to these interior isomers, with the yields of 5-, 4-, 3-, and 2-octacosanone higher by factors of 1.5, 2.2, 4.8, and 10, respectively. This product distribution is consistent with so-called “surface freezing” of linear alkanes where the molecules are preferentially oriented normal to the surface in microscopic particles.

Squalanone isomers with carbonyl groups located adjacent to tertiary carbons are ~5 times enriched relative to those with carbonyl carbons not directly bound to tertiary carbons. Since the initial hydrogen abstraction step is not expected to occur more rapidly for these “α-carbons,” this preference is likely due to more efficient hydrogen abstraction by β-alkoxy radicals compared to α-alkoxy radicals. This hydrogen abstraction is either intra- (i.e., isomerization) or intermolecular (i.e. chain propagation). As both these pathways compete with the reaction of alkoxy radicals with O_2 to form a ketone, it could explain the observed preference for α-ketones. Further evidence for the importance of isomerization reactions in this system is observed by oxidation products containing two oxygen atoms, some of which were second-generation products but others, containing hydroxyl groups, were formed after a single reaction with OH.

Finally, substantial abundances of fragmentation products are observed for squalane, but are much less prevalent for octacosane particles. The only octacosane-derived fragmentation products observed are *n*-carboxylic acids, exhibiting an even-number preference suggesting that cleavage of the second C-C bond is more favorable than the terminal C–C bond. The majority of squalane fragmentation products are formed by cleaving C–C bonds involving tertiary carbons. It is therefore likely that the lack of such carbons (i.e., branching points) in *n*-octacosane is at least partially responsible for the small quantity of observed fragmentation products. This work begins to unravel the complex interplay of molecular structure and particle phase in the heterogeneous oxidation of organic aerosol by OH.

Acknowledgments: K.R.W. and C.R.R. are partially supported by the Department of Energy Office of Science Early Career Research Program. This work was supported by the Laboratory Directed Research and Development Program of Lawrence Berkeley National Laboratory under U.S. Department of Energy Contract No. DE-AC02-05CH11231. C.D.C and K.R.K. are supported by the National Science Foundation under award ATM- 1151062.

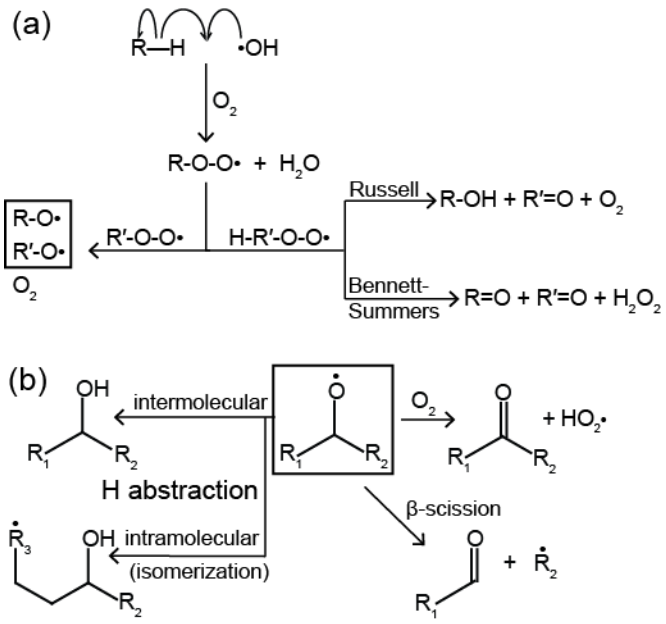

Figure 1. The OH-initiated hydrocarbon oxidation mechanism in the absence of NO_x. Alkoxy radicals are indicated by boxes. (a) Hydrogen abstraction followed by rapid reaction with O_2 produces a peroxy radical, which can react with another peroxy radical either to form an alcohol and a ketone (the Russell mechanism) or two ketones (the Bennett-Summers mechanism), or form two alkoxy radicals. (b) Alkoxy radicals decompose either via H-abstraction (which can be inter- or intramolecular), undergo β-scission, or react with O_2 to form a ketone.

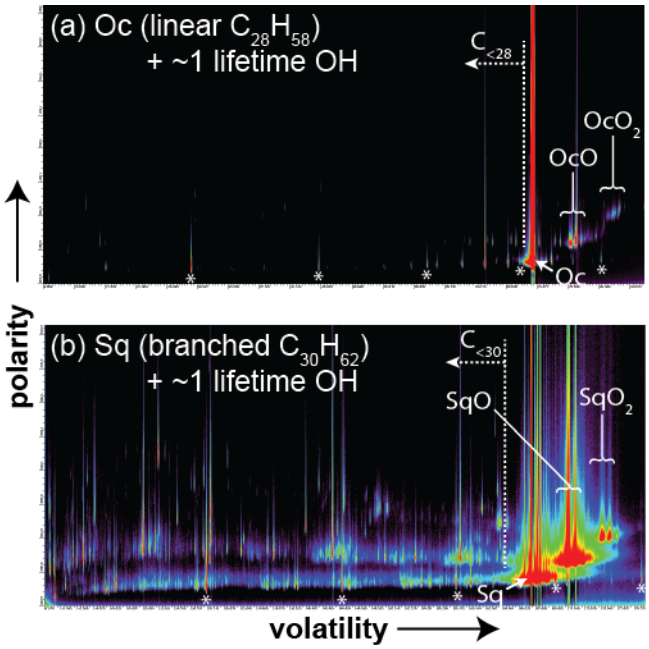

Figure 2. GC×GC EI chromatograms of (a) octacosane (Oc) and (b) squalane (Sq) particles after ~1 oxidation lifetime (OH exposures of 2.7×10^{12} and 5.7×10^{11} molec cm^{-3} s, respectively). Internal standards are labeled "*", and the vertical dotted line separates products that formed via C-C bond scission of the parent (i.e., fragmentation products, to the left) from those that did not (i.e., functionalization products, to the right). Regions with one (OcO, SqO) and two (OcO_2, SqO_2) carbonyl groups added to parent compound are indicated.

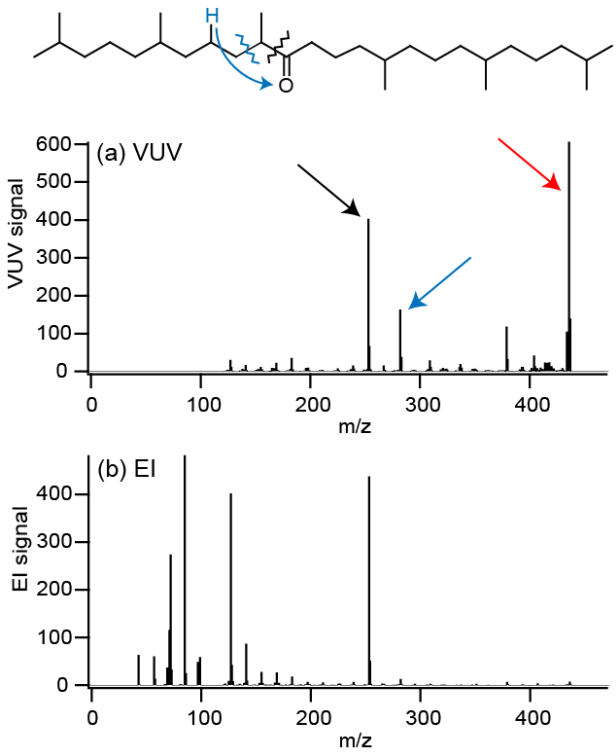

Figure 3. Comparison of mass spectra for squalan-11-one, a first-generation product of the squalane + OH reaction. (a) VUV (10.5 eV, i.e., soft) ionization. A large signal is seen for the parent ion (m/z=436, red), and relatively few fragments are seen, including an acylium ion (black) and a McLafferty rearrangement product (blue). (b) EI (70 eV, i.e., hard) ionization. Essentially no parent ion is observed, and most of the signal is on much smaller mass fragments that provide less information on the molecular structure.

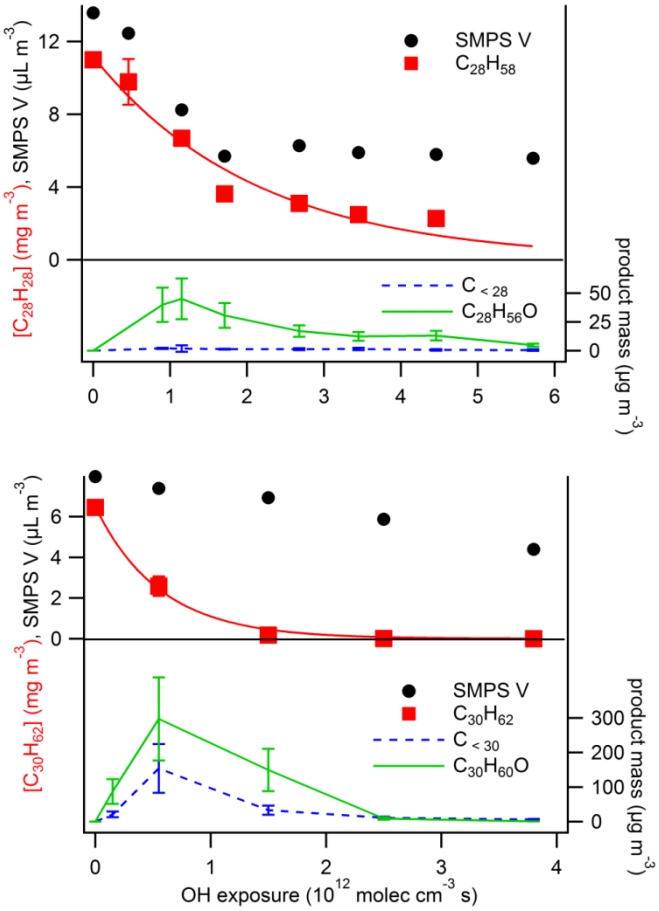

524

525 Figure 4. SMPS volume and GC/MS-derived mass concentrations of parent and product
526 compounds for (a) octacosane (Oc) and (b) squalane (Sq) particles as a function of OH exposure.
527 For parent compounds (red), mass concentrations depict the decay of the EI signal normalized to
528 the scanning mobility particle sizer (SMPS) volume at an OH exposure of 0, assuming a density
529 of 0.807 and 0.810 for octacosane and squalane, respectively. Red lines depict best exponential
530 decay fits to the parent compound observations.

531

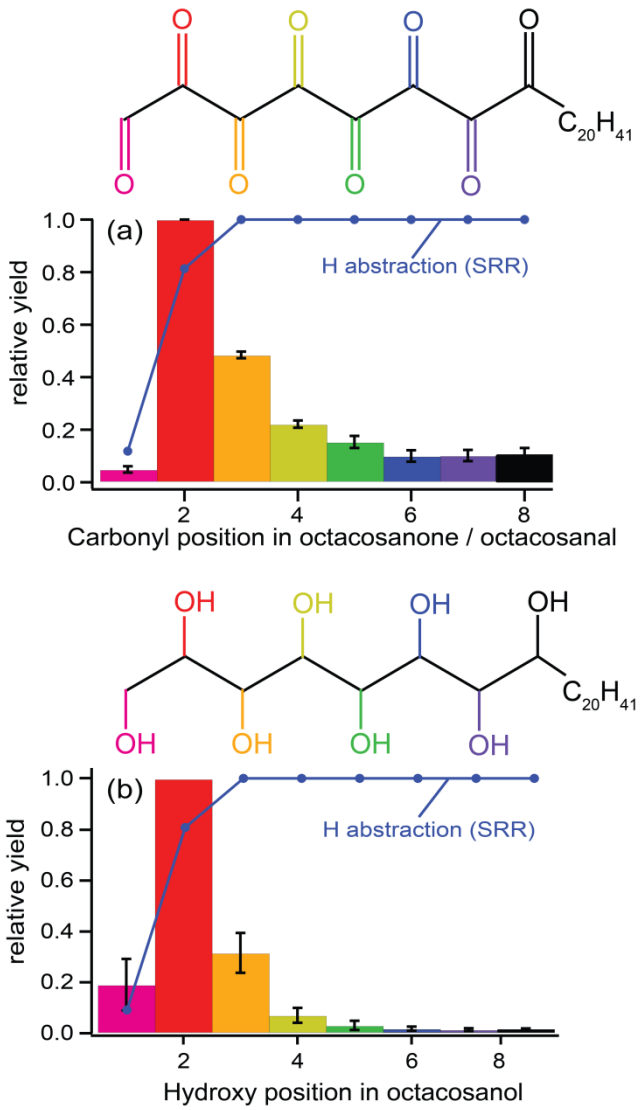

Figure 5. Distribution of positional isomers of octacosane functionalization products. The blue line shows structure-reactivity relationship (SRR) predictions for gas-phase H abstraction.[38] (a) Octacosanone and octacosanal isomers. (b) Octacosanol isomers.

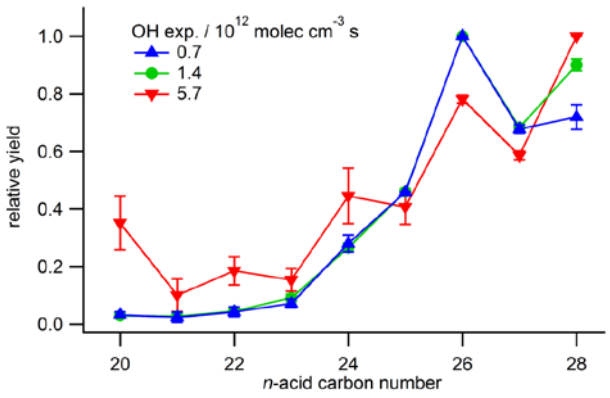

537

538 Figure 6. Distribution of *n*-alkanoic acids in octacosane particles after exposure to gas-phase OH
539 radicals. Error bars indicate the difference in quantifications based on total EI signal and +117
540 ion.

541

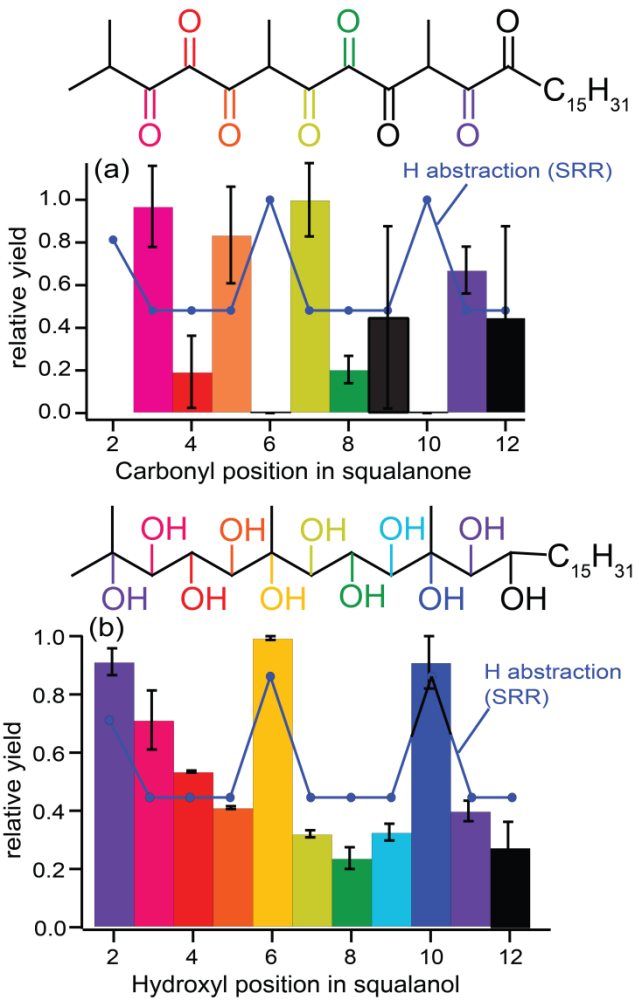

542

543 Figure 7. Distribution of positional isomers of squalane functionalization products. The blue line
544 depicts structure-reactivity relationship (SRR) predictions for gas-phase H abstraction.[38] (a)
545 Squalanone (2,6,10,15,19,23-hexamethyl-tetracosanone) isomers. (b) Squalanol
546 (2,6,10,15,19,23-hexamethyl-tetracosanol) isomers.

547

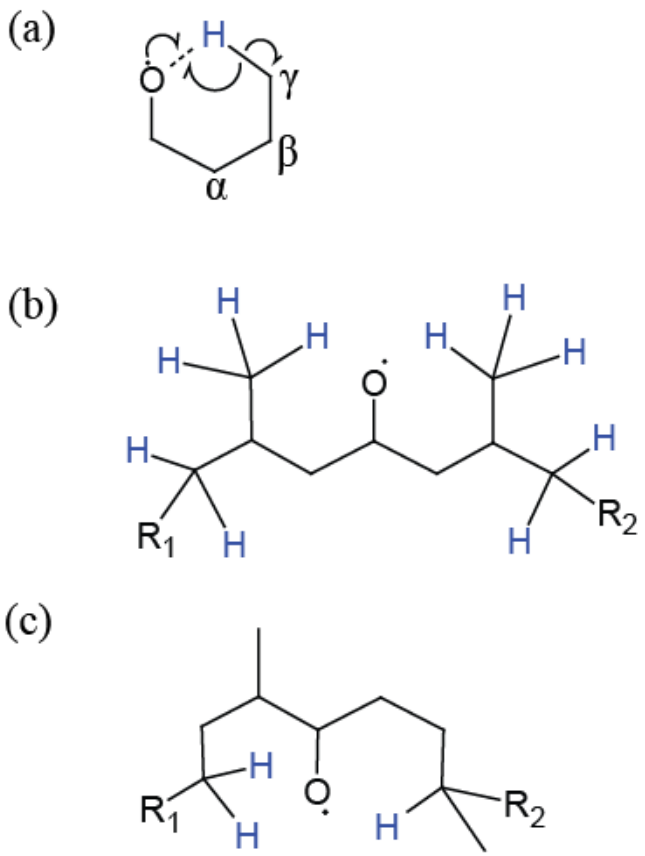

548

549 Figure 8. Reaction of alkoxy radicals via isomerization (a), with potential hydrogen atoms to

550 abstract in blue for (b) β- and (c) α-alkoxy radicals.

551

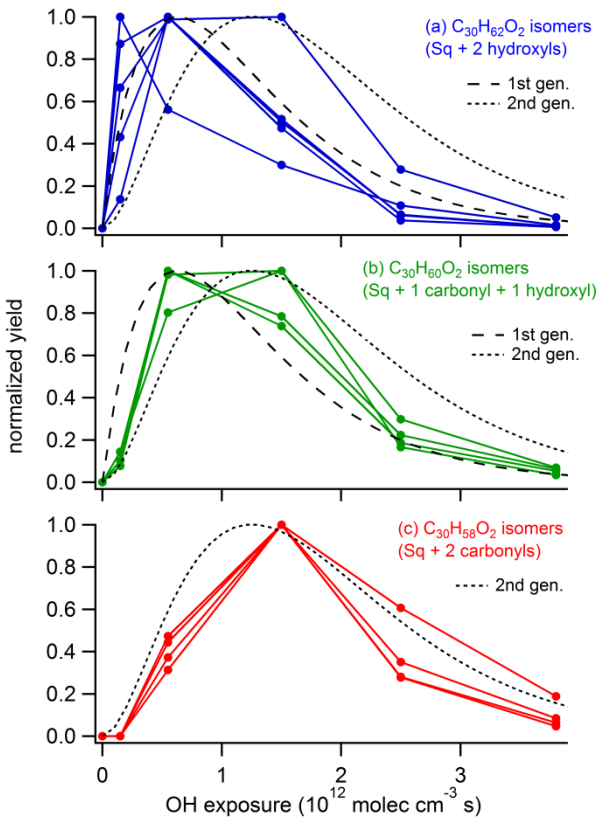

552

553 Figure 9. Normalized yields of $C_{30}H_nO_2$ products (squalane precursor) vs. OH exposure. The
554 dashed lines show the predicted kinetic evolution of first (dashed line) and second (dotted line)
555 generation products.[34] (a) 5 squaladiol isomers. (b) 4 hydroxysqualanol isomers. (c) 4
556 squaladienes isomers. See text for full compound names.

557

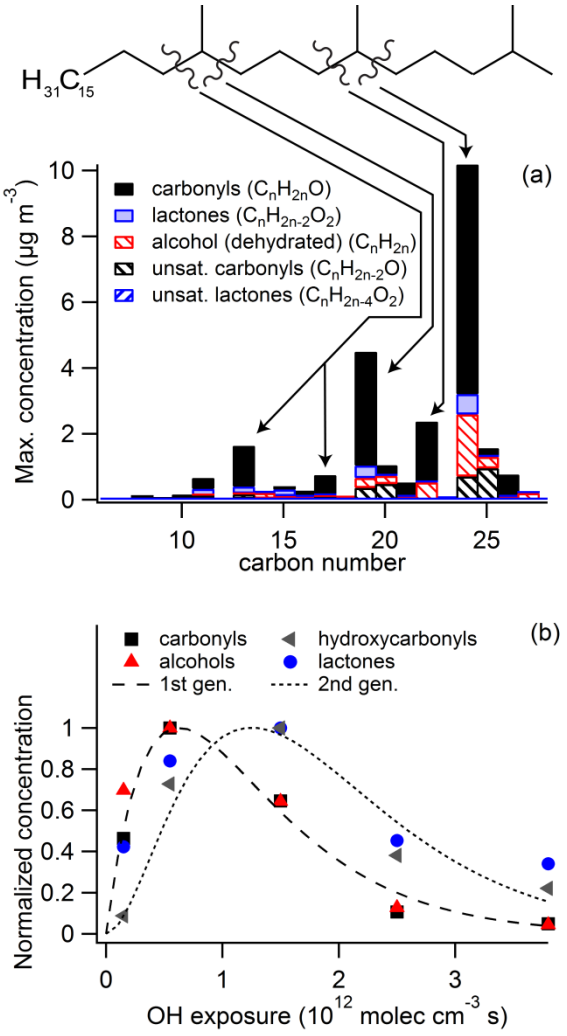

Figure 10. Squalane fragmentation products as a function of: (a) carbon number and (b) OH exposure with dashed lines showing the kinetic evolution of first and second generation products.[34] Shown above the figure is a schematic of the C-C bonds in squalane that are most likely to undergo scission.

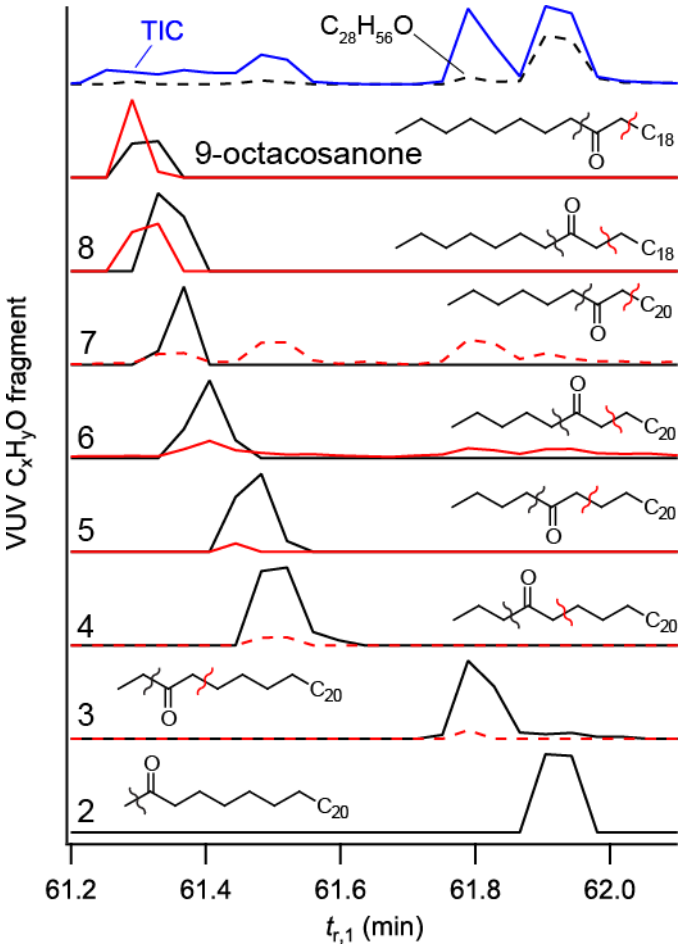

Figure S1. Separation of octacosanone isomers using single-ion VUV chromatograms. Dotted lines indicate a transfer of a hydrogen atom across the C-C bond scission (i.e., a McLafferty rearrangement). The total ion chromatogram (TIC) is of the octacosanone region of the GC×GC chromatogram, and $C_{28}H_{56}O$ is the parent ion.

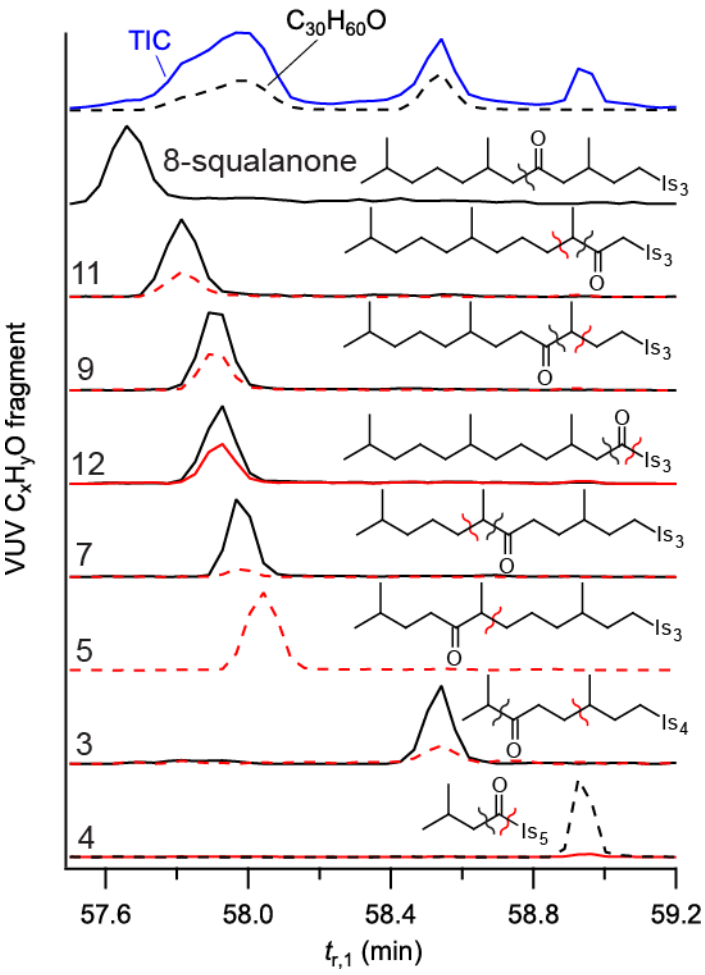

Figure S2. Separation of “squalanone” (2,6,10,15,19,23-hexamethyltetracosanone) isomers using single-ion VUV chromatograms. Dotted lines indicate a transfer of a hydrogen atom across the C-C bond scission (i.e., a McLafferty rearrangement). The TIC is of the squalanone region of the GC×GC chromatogram, and $C_{30}H_{60}O$ is the parent ion. “Is” indicates a C_5H_8 (“isoprene”) unit.

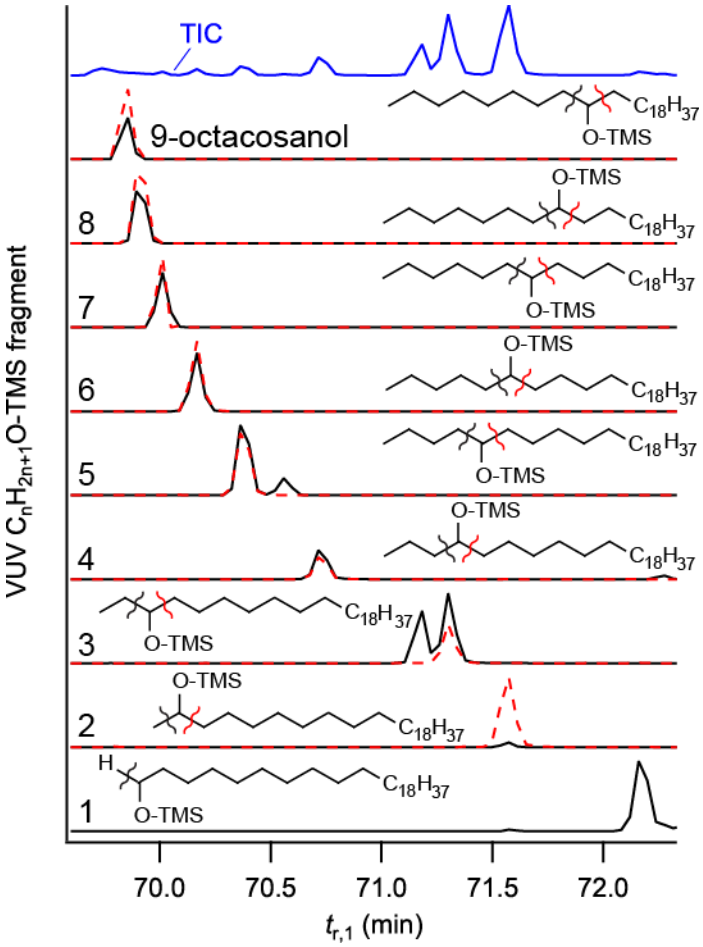

576

577 Figure S3. Separation of octacosanol isomers using single-ion VUV chromatograms w/MSTFA
578 derivatization (which replaces –OH groups with –O-TMS). In VUV, fragmentation tends to
579 break either C-C bond involving the functionalized carbon atom. The TIC is of the octacosanol
580 region of the GC×GC chromatogram.

581

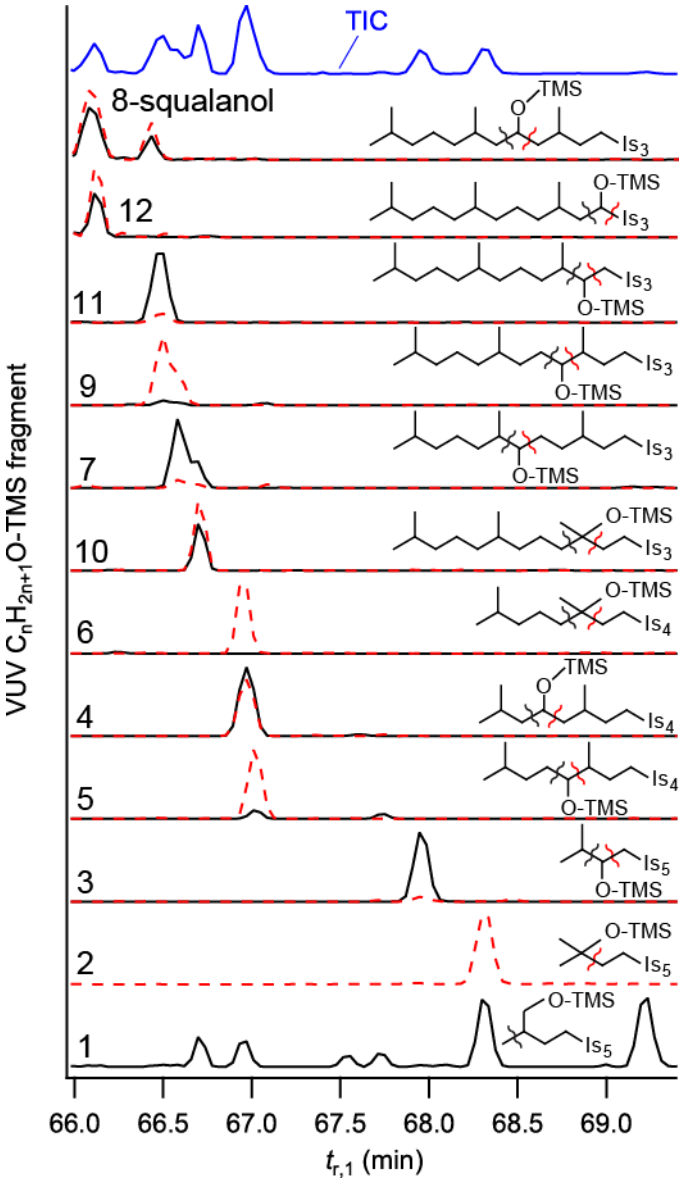

582

583 Figure S4. Separation of "squalanol" (2,6,10,15,19,23-hexamethyltetracosanol) isomers using
584 single-ion VUV chromatograms w/MSTFA derivatization (which replaces –OH groups with –O-
585 TMS). In VUV, fragmentation tends to break either C-C bond involving the functionalized
586 carbon atom. The TIC is of the squalanol region of the GC×GC chromatogram. "Is" indicates a
587 C_5H_8 ("isoprene") unit.

588

References

1. Atkinson, R.; Baulch, D. L.; Cox, R. A.; Crowley, J. N.; Hampson, R. F.; Hynes, R. G.; Jenkin, M. E.; Rossi, M. J.; Troe, J., *Atmos. Chem. Phys.* **2006,** *6*, 3625-4055.
2. Russell, G. A., *J. Am. Chem. Soc.* **1957,** *79*, 3871-3877.
3. Bennett, J. E.; Summers, R., *Can. J. Chem.* **1974,** *52* (8), 1377-1379.
4. Atkinson, R., *Int. J. Chem. Kinet.* **1997,** *29* (2), 99-111.
5. Carter, W. P. L.; Darnall, K. R.; Lloyd, A. C.; Winer, A. M.; Pitts, J. N., *Chem.. Phys. Lett.* **1976,** *42* (1), 22-27.
6. Eberhard, J.; Muller, C.; Stocker, D. W.; Kerr, J. A., *Environ. Sci. Technol.* **1995,** *29* (1), 232-241.
7. Kwok, E. S. C.; Arey, J.; Atkinson, R., *J. Phys. Chem.* **1996,** *100* (1), 214-219.
8. Aschmann, S. M.; Arey, J.; Atkinson, R., *J. Phys. Chem. A* **2001,** *105* (32), 7598-7606.
9. Finlaysonpitts, B. J.; Ezell, M. J.; Pitts, J. N., *Nature* **1989,** *337* (6204), 241-244.
10. Molina, M.; Tso, T.; Molina, L.; Wang, F., *Science* **1987,** *238* (4831), 1253-1257.
11. Finlayson-Pitts, B. J., *Phys. Chem. Chem. Phys.* **2009,** *11* (36), 7760-7779.
12. Hallquist, M.; Wenger, J. C.; Baltensperger, U.; Rudich, Y.; Simpson, D.; Claeys, M.; Dommen, J.; Donahue, N. M.; George, C.; Goldstein, A. H.; Hamilton, J. F.; Herrmann, H.; Hoffmann, T.; Iinuma, Y.; Jang, M.; Jenkin, M. E.; Jimenez, J. L.; Kiendler-Scharr, A.; Maenhaut, W.; McFiggans, G.; Mentel, T. F.; Monod, A.; Prevot, A. S. H.; Seinfeld, J. H.; Surratt, J. D.; Szmigielski, R.; Wildt, J., *Atmos. Chem. Phys.* **2009,** *9* (14), 5155-5236.
13. George, I. J.; Abbatt, J. P. D., *Atmos. Chem. Phys.* **2010,** *10* (12), 5551-5563.
14. Bertram, A. K.; Ivanov, A. V.; Hunter, M.; Molina, L. T.; Molina, M. J., *J. Phys. Chem. A* **2001,** *105* (41), 9415-9421.
15. Cooper, P. L.; Abbatt, J. P. D., *J. Phys. Chem.* **1996,** *100* (6), 2249-2254.
16. Kessler, S. H.; Nah, T.; Daumit, K. E.; Smith, J. D.; Leone, S. R.; Kolb, C. E.; Worsnop, D. R.; Wilson, K. R.; Kroll, J. H., *J. Phys. Chem. A* **2012,** *116* (24), 6358-6365.
17. Kessler, S. H.; Smith, J. D.; Che, D. L.; Worsnop, D. R.; Wilson, K. R.; Kroll, J. H., *Environ. Sci. Technol.* **2010,** *44* (18), 7005-7010.
18. McNeill, V. F.; Yatavelli, R. L. N.; Thornton, J. A.; Stipe, C. B.; Landgrebe, O., *Atmos. Chem. Phys.* **2008,** *8* (17), 5465-5476.
19. Lambe, A. T.; Zhang, J. Y.; Sage, A. M.; Donahue, N. M., *Environ. Sci. Technol.* **2007,** *41* (7), 2357-2363.

20. George, I. J.; Vlasenko, A.; Slowik, J. G.; Broekhuizen, K.; Abbatt, J. P. D., *Atmos. Chem. Phys.* **2007,** *7* (16), 4187-4201.
21. Hearn, J. D.; Smith, G. D., *Geophys. Res. Lett.* **2006,** *33* (17).
22. Liu, C.-L.; Smith, J. D.; Che, D. L.; Ahmed, M.; Leone, S. R.; Wilson, K. R., *Phys. Chem. Chem. Phys.* **2011,** *13* (19), 8993-9007.
23. Choo, K. Y.; Benson, S. W., *Int. J. Chem. Kinet.* **1981,** *13* (9), 833-844.
24. Molina, M.; Ivanov, A.; Trakhtenberg, S.; Molina, L., *Geophys. Res. Lett.* **2004,** *31* (22), 1-5.
25. Vlasenko, A.; George, I. J.; Abbatt, J. P. D., *J. Phys. Chem. A* **2008,** *112* (7), 1552-1560.
26. Docherty, K. S.; Ziemann, P. J., *J. Phys. Chem. A* **2006,** *110* (10), 3567-3577.
27. Knopf, D. A.; Mak, J.; Gross, S.; Bertram, A. K., *Geophys. Res. Lett.* **2006,** *33* (17).
28. Eliason, T. L.; Gilman, J. B.; Vaida, V., *Atmos. Environ.* **2004,** *38* (9), 1367-1378.
29. Hearn, J. D.; Renbaum, L. H.; Wang, X.; Smith, G. D., *Phys. Chem. Chem. Phys.* **2007,** *9* (34), 4803-4813.
30. Renbaum, L. H.; Smith, G. D., *Phys. Chem. Chem. Phys.* **2009,** *11* (14), 2441-2451.
31. Kroll, J. H.; Smith, J. D.; Che, D. L.; Kessler, S. H.; Worsnop, D. R.; Wilson, K. R., *Phys. Chem. Chem. Phys.* **2009,** *11* (36), 8005-8014.
32. Smith, J. D.; Kroll, J. H.; Cappa, C. D.; Che, D. L.; Liu, C. L.; Ahmed, M.; Leone, S. R.; Worsnop, D. R.; Wilson, K. R., *Atmos. Chem. Phys.* **2009,** *9* (9), 3209-3222.
33. Huff Hartz, K. E.; Weitkamp, E. A.; Sage, A. M.; Donahue, N. M.; Robinson, A. L., *Journal of Geophysical Research: Atmospheres* **2007,** *112* (D4), n/a-n/a.
34. Wilson, K. R.; Smith, J. D.; Kessler, S. H.; Kroll, J. H., *Phys. Chem. Chem. Phys.* **2012,** *14* (4), 1468-1479.
35. Worsnop, D.; Morris, J.; Shi, Q.; Davidovits, P.; Kolb, C., *Geophys. Res. Lett.* **2002,** *29* (20), 1-4.
36. Heslot, F.; Cazabat, A. M.; Levinson, P., *Phys. Rev. Lett.* **1989,** *62* (11), 1286-1289.
37. Koop, T.; Bookhold, J.; Shiraiwa, M.; Poschl, U., *Physical Chemistry Chemical Physics* **2011,** *13* (43), 19238-19255.
38. Kwok, E. S. C.; Atkinson, R., *Atmos. Environ.* **1995,** *29* (14), 1685-1695.
39. Isaacman, G.; Chan, A. W. H.; Nah, T.; Worton, D. R.; Ruehl, C. R.; Wilson, K. R.; Goldstein, A. H., *Environ. Sci. Technol.* **2012,** *46* (19), 10632-10640.
40. Earnshaw, J. C.; Hughes, C. J., *Phys. Rev. A* **1992,** *46* (8), R4494-R4496.
41. Harris, J. G., *J. Phys. Chem.* **1992,** *96* (12), 5077-5086.
42. Xia, T.; Landman, U., *J. Chem. Phys.* **1994,** *101* (3), 2498-2507.
43. Lim, Y. B.; Ziemann, P. J., *Environmental Science & Technology* **2009,** *43* (7), 2328-2334.